Food Research International 133 (2020) 109164

Contents lists available at ScienceDirect

Food Research International

journal homepage: www.elsevier.com/locate/foodres

Novel Amadori and Heyns compounds derived from short peptides found in dried cocoa beans

Paweł J. Andruszkiewicz[a], Roy N. D'Souza[a], Marcello Corno[b], Nikolai Kuhnert[a,*]

[a] Department of Life Sciences and Chemistry, Jacobs University Bremen, Campus Ring 1, 28759 Bremen, Germany
[b] Barry Callebaut AG, Westpark, Pfingstweidstrasse 60, Zurich 8005, Switzerland

ARTICLE INFO

Keywords:
Cocoa
Maillard reaction
Amadori compounds
Heyns compounds
HPLC-MS
Tandem MS
PCA

ABSTRACT

Chemical transformations of Amadori compounds are responsible for the formation of aroma volatiles at the end of the Maillard reaction cascade, which in turn contributes to unique organoleptic characteristics of chocolate. A large amount of short peptides reported in fermented cocoa suggests the existence of a much larger variety of these flavor precursors than previously suspected. An HPLC-MS-MS study was performed on dried Malaysian cocoa beans to identify novel Amadori and Heyns compounds. In total, 34 species were found, including 26 previously unknown derived from di- and tripeptides. We illustrate how the structures were elucidated via tandem MS experiments, as well as present a comparative study on their relative quantities in samples coming from 11 countries of origin. There were significant differences between them, and discrimination was possible by principal component analysis based on Amadori content alone. However, the PCA separation could be a result of various post-harvest practices exerted among said countries.

1. Introduction

Chocolate production, from the bean to the factory, involves many processes, which involve slight to drastic elevations of the temperature. During cocoa beans fermentation, the temperature reaches approximately 50 °C (Lagunes Gálvez, Loiseau, Paredes, Barel, & Guiraud, 2007; Camu et al., 2008). Although it is difficult to establish it for traditional drying methods such as sun-drying, artificial drying is performed at roughly 60 °C (Rodriguez-Campos et al., 2012). Roasting takes place under the roughest conditions, with the final temperature reaching between 110 and 140 °C (Beckett, 2009). Increasing the intensity of thermal treatment lets the cocoa develop its extraordinary character. Paired with its unique composition, it enables many intricate chemical reactions to occur. Most prominently, the Maillard reaction, which starts with transformations arising from the reaction of amino acids or peptides and sugars. It can be initiated even at room temperature; however, it becomes dominant in temperatures above 100 °C (Ruan, Wang, & Cheng, 2018). It has an enormous effect on the organoleptic properties of foods as it produces many aroma volatiles as well as colored polymers (Yaylayan, 2003). Hence, it is important to the food industry as it influences the product quality of heated foods (Ames, 1990, 1998). The first major stable compounds of the Maillard reaction are Amadori and Heyns compounds, condensation, and rearrangement products of amino acids with either glucose or fructose, respectively. They are of most importance as their thermal degradation directly leads to the formation of aroma compounds and melanoidins (brown pigments). They are very well studied in model systems (Hofmann & Schieberle, 2000; Davidek, Clety, Aubin, & Blank, 2002) as well as they were detected in some foods (Meitinger, Hartmann, & Schieberle, 2014; Yuan, Sun, Chen, & Wang, 2016, 2017). Additionally, they have gained much attention after the discovery of their formation in physiological conditions and their involvement in the generation of advanced glycosylation end products (AGEs) (Singh, Barden, Mori, & Beilin, 2001; Horvat & Jakas, 2004). More importantly, Amadori compounds of dipeptides were found in model systems. It was shown that their degradation produces more variety of pyrazines than their amino acid counterparts (Zou, Liu, Song, & Liu, 2018). Hence, the importance of studying them in an actual food matrix arises. So far, there were only a few single amino acids Amadori compounds identified in cocoa (Meitinger et al., 2014). However, taking into account many short peptides found across cocoa fermentation (D'Souza et al., 2018) and the mild conditions needed to generate Amadori compounds, more variety should exist in the raw material for chocolate production. Thus, we present an HPLC-MS-MS study on Malaysian cocoa beans, which aimed to identify more novel Amadori compounds in dried cocoa beans. Additionally, for the first time, we present a comparative analysis of relative quantities of Amadori compounds in different cocoa samples. This research can help with differentiation as well as establishing

* Corresponding author at: Department of Life Sciences & Chemistry, Jacobs University Bremen gGmbH, Campus Ring 1, 28759 Bremen, Germany.
E-mail address: n.kuhnert@jacobs-university.de (N. Kuhnert).

https://doi.org/10.1016/j.foodres.2020.109164
Received 6 December 2019; Received in revised form 9 March 2020; Accepted 15 March 2020
Available online 29 March 2020

quality standards for dried cocoa beans.

2. Material and methods

2.1. Chemicals and reagents

Acetone, dichloromethane, HPLC-grade acetonitrile, HPLC-grade isopropanol, HPLC-grade methanol, and petroleum ether were supplied by Carl Roth (Germany). Acetic acid, formic acid, hesperetin, and sodium hydroxide were supplied by Sigma-Aldrich (Germany). Milli-Q water (18.2 MΩ•cm at 25 °C) was used in all the experiments performed.

2.2. Sample collection and preparation

A sample of fermented and dried cocoa from Malaysia (internally labeled as MC01) was supplied by Barry Callebaut AG. This sample was used for the tandem MS identification of novel Amadori compounds. It was taken from a farm near Kuala Lipis, Malaysia, and belonged to the PBC 123 clone. It was harvested as a part of the main crop in January 2016. The cocoa beans were fermented for 144 h and then dried for 96 h. After the shipment, the sample was stored at 4 °C before any processing.

There were thirteen additional samples obtained by Barry Callebaut AG in order to perform relative quantification of Amadori compounds and discriminant analysis. They came from: Brazil (BC03), Cameroon (PC20), Dominican Republic (E2), two from Ghana (PD04 and PD08), Indonesia (IA03), two from Ivory Coast (PD07 and PD11), Java (PC23), Madagascar (PC21), Papua New Guinea (PC18), Nigeria (NE01), and San Thome (PC19). The Brazilian sample (BC03, CCN-51 hybrid) was harvested on Copa70 estate (GPS 14° 02′ 53″S, 039 °23′ 02″W), and within 12 h, the fermentation was started. The beans were fermented for 6 days and directly after sun-dried. It was noted that the crop yield and quality was poor because of a very dry period at that time. The sample from Indonesia (IA03, TSH 858 hybrid) was obtained from Pt Bumiloka estate near Sukabumi, Jakarta. The beans were fermented 12 h within harvest, which lasted for 6 days, followed by 7 days of sun-drying. The post-harvest treatment of the remaining samples is unknown.

Approximately 30 g of cocoa beans from each sample were deshelled and ground to a fine powder using a knife mill (Retsch Grindomix GM200, Germany) at 10,000 rpm. Obtained ground powder was stored at 4 °C until further processing. The powder was defatted for 8 h using petroleum ether as an extraction solvent in an automated Soxhlet extraction apparatus (Büchi B-811, Germany). The defatted powder was dried under vacuum and stored at 4 °C until further use.

2.3. Extraction

Extraction of the sample for Amadori compound identification as well as relative quantification of both Amadori compounds and oligopeptides was performed according to a previously established protocol (D'Souza et al., 2018). 5 mL of extraction buffer (MeOH:-H_2O:CH_3COOH::70:28:2) was added to 50 mg of defatted cocoa powder, mixed and sonicated in an ultrasonic bath for 10 min, then stirred for 30 min, and finally filtered through a PTFE syringe membrane filter (0.45 μm). The obtained extract was spiked with hesperetin as an internal standard (final concentration of 2 mg/L) and directly used for HPLC-MS experiments.

2.4. HPLC-TOF-MS-MS measurements

HPLC separation conditions for every experiment were adapted from a previously established method (D'Souza et al., 2018). Agilent 1260 HPLC system equipped with a Poroshell 120 EC-C18 column (RRHD, 2.1 × 100 mm, 2.7 μm particle size) was used. Milli-Q water and acetonitrile with the addition of 0.05% of formic acid were used as Solvent A and Solvent B, respectively. The sample injection volume employed was 2 μL. The flow rate was constant at 0.4 mL/min, and the column oven temperature was set up to 40 °C. The chromatographic gradient used for the analysis was as follows: (t (min), %B): (0, 8); (1, 8); (2.5, 12); (8, 16.5); (9, 17); (10, 17.5); (11, 17.5); (12, 18.5); (13, 18.5); (23, 95); (28, 95). The above-mentioned HPLC system was coupled to an Impact HD ultra-high resolution ESI-Q-q-TOF mass spectrometer (Bruker Daltonics, Bremen, Germany) with an electrospray ionization source (nebulizer pressure of 1.8 bars, dry gas flow rate of 9 L/min, and dry gas temperature of 200 °C). The data were acquired in positive ion mode and reported NIST monoisotopic atomic masses of the elements (Coursey, Schwab, Tsai, & Dragoset, 2015) were used to calculate monoisotopic molecular masses of detected compounds. 0.1 M sodium formate solution was used to calibrate the TOF analyzer before each sample measurement. During the MS-MS measurements, the collision energy was set to change dynamically and was proportional to the mass of the fragmented molecule. The MS relative quantification of Amadori compounds was performed using Bruker QuantAnalysis software, whereas the peptides using a previously established protocol (D'Souza et al., 2018). In both cases, all samples were normalized using a sum of all detected MS peaks.

2.5. Discriminant analysis

The discriminant analysis of the mass spectrometric data was performed using Orange software (Demsar et al., 2013). InfoGain method was used to rank all the features, and subsequently, the top 14 most discriminant were chosen for the principal component analysis (PCA).

3. Results and discussion

The identification of all of the early Maillard reaction products was performed on a methanolic extract of a fermented and dried Malaysian cocoa beans sample. This country of origin was chosen as Malaysian beans tend to have, on average lower protein content than others. Therefore, the results of the identification can be easily extrapolated to other bean origins. Recent studies have shown a large amount (~800) of previously unknown peptides present in coca (D'Souza et al., 2018). We were able to generate a mass list of hypothetical Amadori compounds derived from those peptides, which we compared with obtained MS data. Examination of tandem mass spectra revealed the presence of thirty-two short-peptide Amadori compounds, surprisingly including Heyns compounds as well (the difference between them is shown in Fig. 1). In cocoa, the amounts of fructose and glucose (0.0–103.4 and 4.3–175.0 mg/100 g of dry mass respectively) is considerably low (Megías-Pérez, Grimbs, D'Souza, Bernaert, & Kuhnert, 2018) in comparison to amino acid content reported for fermented beans in the literature (Rohsius, Matissek, & Lieberei, 2006), which is between 500 and 2520 mg/100 g of dry mass. Moreover, approximate Amadori content amounting to 80 mg/100 g of unroasted beans (Meitinger et al., 2014) makes their discovered diversity even more surprising.

3.1. Identification of novel Amadori compounds

The HPLC-ESI-MS-MS experiments revealed the presence of thirty-two different short-peptide Amadori and Heyns compounds: six derived from amino acids and already known in cocoa (Meitinger et al., 2014), twenty-three dipeptide-containing and three tripeptide-containing compounds which are to our knowledge novel in the food literature. The summary of all the identified structures is shown in Table 1. The novel compounds elucidated in this paper are as follows: Fru-VP (**1**), Fru-FG (**2**), Fru-IA (**3**), Glc-AY or YA or FS or SF (**4**), Fru-FS (**5**), Fru-L(I)G (**6**), Fru-VA (**7**), Fru-L(I)P (**8**), Fru-L(I)V (**9**), Fru-L(I)V or VL(I) (**10**), Glc-WVT (**11**), Fru-TVW (**12**), Glc-TVW (**13**), Fru-IT (**14**), Fru-L(I)L(I) (**15**), Fru-L(I)E (**16**), Fru-FT (**17**), Fru-IF (**18**, **19**), Fru-FL(I) (**20**,

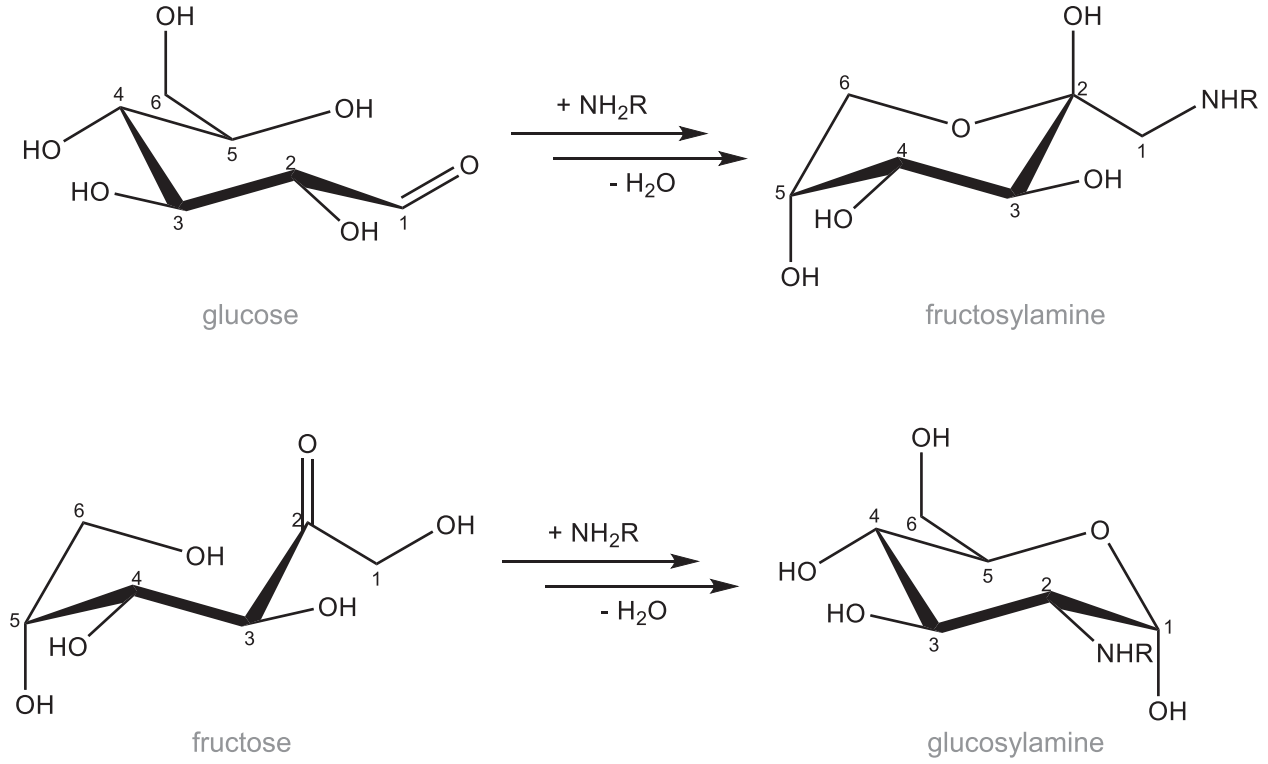

Fig. 1. Difference between Amadori (fructosylamine) and Heyns compounds (glucosylamine), which originate from glucose and fructose, respectively.

21), Glc-VY (**22**), Fru-FE (**23**), Fru-MF (**24**), Fru-VS (**25**), Fru-L(I)S or VT (**26**), Fru-V (**27**). Structures previously described in the literature, which we have detected are: Fru-L(I) (**28**), Fru-M (**29**), Fru-F (**30**), Fru-Y (**31**, **32**). An extracted ion chromatogram of chosen examples of compounds is shown in Fig. 2. After the N-glycosylation of peptides with glucose, the sugar structure resembles fructose (it is opposite for fructose reactions), hence Fru- (fructosyl-) and Glc- (glycosyl-) nomenclature. In some cases, the spectra recorded were ambiguous to an extent, and the absolute assignment of the compounds was not possible. Firstly, in the absence of either Amadori- or Heyns-specific fragmentation peaks (**6**, **10**, **12**, **18**, **19**), we assumed that the compound investigated was an Amadori compound as those should be much more abundant in cocoa. Secondly, in some cases, the sequence of the peptide chain was not clear, and we annotated it accordingly. Additionally, the stereochemistry of the amino acids involved could not be determined, and we assume that all of them are L-isomers. The spectra of all of the compounds are included in the Supplementary Information. Here, we will discuss the general behavior of Amadori and Heyns compounds during tandem MS fragmentation as well as apply our approach to three particular examples.

The tandem MS fragmentation patterns of single amino acid Amadori compounds are known and well understood based on both analytical standards and Maillard reaction model systems (Hau, Devaud, & Blank, 2004; Davidek, Kraehenbuehl, Devaud, Robert, & Blank, 2005; Wang, Lu, Liu, & He, 2008). The distinction between Amadori and Heyns compounds using their specific fragmentation patterns is possible and described in the literature as well (Yuan et al., 2016, 2017). The detection and identification of those species was achieved in number of foods including cocoa, tomatoes, varieties of peppers, asparagus, cauliflowers, carrots, celery, coffee, barley, wheat, garlic, raisins, and jujubes (Eichner, Reutter, & Wittmann, 1993; Meitinger et al., 2014; Yuan et al., 2016, 2017). Moreover, the presence of short peptide-derived Amadori compounds was confirmed in Maillard reaction model systems by mass spectrometry techniques (Mennella, Visciano, Napolitano, Castillo, & Fogliano, 2006; Zou et al., 2018).

Generally, the N-glycosylated amino acids fragment producing ions with characteristic multiple neutral losses of H_2O (up to three) along with consecutive losses of CO_2 and H_2CO as the most abundant peaks. The remaining peaks come from the fragmentation of the amino acid itself, most notably the peak of protonated amino acid $[AA + H]^+$. The distinction between Amadori and Heyns compounds is possible based on unique neutral losses of 96 and 150, which is $[M + H\text{-}2H_2O\text{-}CH_3OH\text{-}CO]^+$ ion specific for Heyns and $[AA\text{-}H + CH_2]^+$ ion specific for Amadori compounds respectively. Another paper describes fragmentation patterns of more complex glycosylated peptides: Amadori compounds of tri- and tetrapeptides, glycopeptide esters, a glycosylamine, and a cyclic Amadori compound (Jeri, Versluis, Horvat, & Heck, 2002). The data reported show each of the compound class fragments similarly, differing only in abundance of specific ions, especially the multiple neutral losses of H_2O as well as losses of CO_2 and H_2CO.

Fig. 3 shows spectra we obtained for following N-glycosylated peptides: a) (**27**) Fru-V, b) (**14**) Fru-IT, and c) (**13**) Glc-TVW. Only peaks with intensity larger than 1% were considered. Fru-V (**27**, *m/z* 280), similarly to other single amino acid Amadori compounds in this investigation, was already studied via mass spectrometry techniques, and its fragmentation pattern is previously known (Hau et al., 2004; Davidek et al., 2005; Wang et al., 2008; Yuan et al., 2016). Furthermore, it is amongst seven Amadori compounds known to cocoa (Meitinger et al., 2014). The most abundant peaks in its fragmentation come from a typical pattern of sugar dehydration and subsequent loss of carbon dioxide or formaldehyde. The parent ion (*m/z* 280) loses an H_2O molecule producing the first fragmentation peak at *m/z* 262, followed by consecutive loss of CO_2 resulting in the *m/z* 234 peak. Similarly, the loss of two water molecules leads to the formation of *m/z* 244 ion, which after the decarboxylation, yields the most abundant daughter ion $[M + H\text{-}2H_2O\text{-}CO]^+$ at *m/z* 216. This compound does not produce a stable $[M + H\text{-}3H2O]^+$ ion, instead forming the cyclic $[M + H\text{-}3H_2O\text{-}CO]^+$ and $[M + H\text{-}3H_2O\text{-}H_2CO]^+$ ions directly, at *m/z* 198 and 196 respectively, which are much less abundant overall. The amino acid component can be cleaved off from the sugar as well, yielding a protonated peptide peak (*m/z* 118), which in turn helps the structure

Table 1
Amadori and Heyns compounds identified in the study. Fru is an abbreviation for fructosyl (Amadori compound), Glc is an abbreviation for glycosyl (Heyns compound). Amino acid names are depicted by their standard single-letter codes. L(I) indicates that the distinction between leucine and isoleucine was not possible.

ID	Compound Identity	RT	Exp. *m/z*	Calc. *m/z*	Error [ppm]	Mol. Formula	Intensity	Ion Fragments
1	Fru-VP	1.1	377.1923	377.1918	1.23	$C_{16}H_{28}N_2O_8$	285,782	216.1242(1 0 0); 341.171(90); 293.1508(76); 359.1811(22); 215.1401(17); 234.1348(12); 116.0718(11); 323.1618 (9); 198.1137(7); 242.1042(6); 227.1424(3); 150.0938(4); 260.1168(2); 128.0728(2)
2	Fru-FG	1.3	385.1606	385.1605	0.25	$C_{17}H_{24}N_2O_8$	177,288	301.1188(1 0 0); 349.138(44); 264.1239(39); 120.0815(31); 331.1282(24); 223.1065(17); 246.1125(16); 313.1165(12); 198.0915(11); 283.1065(7); 367.1477(6); 154.0532(5); 235.0992(2); 289.1188 (1)
3	Fru-IA	0.9	365.1919	365.1918	0.07	$C_{15}H_{28}N_2O_8$	518,548	281.1508(1 0 0); 230.1396(51); 329.1721(49); 86.0978(20); 311.1598(20); 212.128(17); 203.1402(10); 347.1825(9); 164.1083(8); 168.0653(7); 168.0653(7); 293.1525 (5); 248.1484(3); 215.1389(3); 263.1394(3)
4	Glc-AY or YA or FS or SF*	1.3	415.1713	415.1711	0.40	$C_{18}H_{26}N_2O_9$	55,928	331.1294(1 0 0); 361.139(25); 379.1522(17); 166.0855(14); 235.1066(14); 253.1187(12); 207.1124(10); 120.0814(9); 343. 1279(9); 315.1322(8); 244.0982(8); 292.1207(7); 313.1161(7); 397.1602(4); 285.1216(4); 319.1261(3); 265.1177(1)
5	Fru-FS	0.9	415.1712	415.1711	0.13	$C_{18}H_{26}N_2O_9$	114,360	331.1296(1 0 0); 379.15(43); 264.1224(25); 120.0812(15); 361.1402(15); 246.1132(10); 253.1178(8); 198.0934(8); 232.0813(7); 343.1319(6); 285.1240(6); 397.1593(5); 265.1239(5); 136.0773(5); 313.1175(4); 292.1218(2)
6	Fru-L(I)G**	0.9	351.1760	351.1762	−0.41	$C_{14}H_{26}N_2O_8$	339,452	267.1356(1 0 0); 230.1394(38); 315.1562(36); 297.1448(23); 86.098(22); 212.1295(14); 164.1087(8); 333.1672(7); 189.1250(7); 154.0448(6); 279.1338(5); 249.1229(4); 220.0839(4); 202.0736(4)
7	Fru-VA	0.7	351.1768	351.1762	1.61	$C_{14}H_{26}N_2O_8$	322,514	267.1356(1 0 0); 216.1235 (44); 230.1394(38); 315.1562(36); 297.1448(23); 86.098(22); 212.1295(14); 150.0931 (14); 164.1087(8); 198.1139(8); 333.1672(7); 189.1250(7); 279.1338(5); 168.0657 (5); 129.1031(5); 249.1229(4); 220.0839(4); 202.0736(4); 234.1004 (3); 201.1245(2)
8	Fru-L(I)P	2.1	391.2066	391.2075	−2.26	$C_{17}H_{30}N_2O_8$	92,296	309.1814(1 0 0); 230.139(58); 307.1658(57); 355.1883(53); 357.2017(33); 216.1234(28); 339.1901(24); 212.1241(14); 150.0917(13); 225.1611(12); 116.0704(11); 373.1955(11); 248.1509(11); 229.1565(10); 337.1784(7); 258.1364(7); 86.0981(7); 276.1435(6); 164.1073(6); 132.1032(6); 276.1435 (5); 198.1141(4); 291.1712(3); 241.1559(3)
9	Fru-L(I)V	1.3	393.2229	393.2231	−0.55	$C_{17}H_{32}N_2O_8$	95,486	309.1819(1 0 0); 230.1383(69); 357.2024(49); 86.0977(26); 339.1913(24); 355.1852(21); 375.2125(13); 231.1694(13); 196.1299(12); 164.1081(12); 212.1281(11); 129.1042(9); 263.1725(6); 248.1532 (6); 226.1087(6); 132.1036(6); 243.1719(2)
10	Fru-L(I)V or VL(I)**	2.0	393.2237	393.2231	1.54	$C_{17}H_{32}N_2O_8$	200,348	309.1812(1 0 0); 357.2036(36); 216.1223(31); 230.1396(30); 339.1908(23); 355.1868(19); 307.1673(18); 231.1695(10); 210.1136(9); 198.1140(9); 375.2151(7); 150.0935(6); 321.1767(4); 291.1750(4); 263.1801(4); 164.1066(3); 86.0968(3)
11	Glc-WVT*	4.3	567.2647	567.2661	2.47	$C_{20}H_{28}N_4O_5$	26,832	283.0826(1 0 0); 258.1153(96); 240.1019(89); 217.0505(81); 513.2342(55); 384.1935(49); 257.1143(46); 321.1462(39); 366.18(37); 303.13(36); 388.1881(29); 267.117(29); 564.2985(26); 402.1727(25); 483.2169(25); 336.1712(25); 531.2508(23); 286.1599(22); 495.2273(21); 258.1587(20); 549.2571(18); 412.2026(16); 461.1362(10); 102.0561(9); 188.0704(8); 430.1996(8); 156.076(8); 120.0697(8); 306.1531(7); 405.2088(7); 471.2283(2)
12	Fru-TVW**	5.9	567.2658	567.2661	0.53	$C_{20}H_{28}N_4O_5$	28,330	281.1496(1 0 0); 317.1723(98); 483.2216(90); 302.0995(67); 279.1356(66); 304.1649(65); 265.1201(65); 299.163(64); 513.2355(55); 309.1476(49); 251.1387(46); 373.1733(36); 469.2047(34); 355.16(32); 205.1007(31); 237.1232(31); 345.1648(28); 327.1567(27); 305.1695(24); 173.1276(16); 201.1222(15); 188.0715(14); 531.246(12); 549.251(12); 159.0892(7); 102.0576(7); 405.2048(1)
13	Glc-TVW*	5.8	567.2648	567.2661	2.29	$C_{20}H_{28}N_4O_5$	24,936	304.1678(1 0 0); 299.1614(99); 483.2264(85); 265.1193(85); 279.1357(79); 281.1514(79); 251.1376(66); 317.1708(54); 309.1462(53); 205.0991(42); 469.2109(41); 237.1267(31); 327.1538(30); 513.2293(27); 136.0746(26); 305.171(25); 345.1654(24); 173.1305(15); 219.1177(15); 107.0516(15); 363.1836(13); 549.2705(11); 451.1959(10); 531.2362(9); 409.1762(9); 102.0569(8); 471.2253(6); 405.2123(5)
14	Fru-IT	0.8	395.2024	395.2024	0.00	$C_{16}H_{31}N_2O_9$	189,550	311.1595(1 0 0); 359.1819(50); 86.0976(49); 230.1393(46); 341.1708(17); 233.15(10); 136.0758(9); 212.1311(7); 132.1047(6); 323.1643(6); 198.0776(6); 173.1296(6); 248.1505(5); 164.1069(5); 293.1476(5); 276.1469(4); 377.1927(4); 96.0445(3); 147.0792(2); 264.1149(2); 245.1533(1)
15	Fru-L(I)L(I)	3.9	407.2393	407.2388	−1.23	$C_{18}H_{35}N_2O_8$	103,464	323.1973(1 0 0); 230.1388(41); 371.2179(38); 353.2073(24); 127.0399(23); 86.0978(19); 145.0508(18); 103.0398(15); 210.1128(11); 389.23(11); 303.0877(11); 164.1078(10); 196.136(9); 258.1344(9); 212.1289(8); 245.1863(8); 248.1493(7); 97.0291(7); 276.1433(5); 120.0824(4); 257.1863(3)
16	Fru-L(I)E	0.8	423.1978	423.1973	−1.18	$C_{17}H_{31}N_2O_{10}$	420,024	339.1561(1 0 0); 387.1771(49); 230.1392(31); 369.1655(23); 261.1451(14); 86.0982(14); 212.1286(9); 405.1878(8); 274.0909(7); 248.1473(6); 196.1326(6); 321.1442(5); 164.1065(4); 273.1411(3); 148.0619(3); 185.1306(2)
17	Fru-FT	1.0	429.1868	429.1868	0.00	$C_{19}H_{29}N_2O_9$	101,052	345.1445(1 0 0); 393.1679(32); 427.2574(29); 264.1244(19); 327.1322(19); 120.0826(16); 375.1562(15); 246.1079(13); 267.1355(13); 217.1554(11); 411.1759(10); 228.1024(7); 198.0765(7); 86.0964(5); 129.1029(5); 103.0404(4); 292.0312(4); 279.1412(3)
18	Fru-IF**	5.0	441.2235	441.2231	0.74	$C_{21}H_{32}N_2O_8$	79,852	357.1811(1 0 0); 405.2012(36); 230.1395(32); 387.1892(19); 279.1714(9); 244.0987(8); 86.0972(8); 212.13(8); 423.2144(8); 164.1084(6); 292.1182(6); 311.176(5); 196.1352(5); 120.0826(4); 369.1843(3); 136.0777(2); 194.1207(2)
19	Fru-IF**	6.1	441.2214	441.2231	−3.93	$C_{21}H_{32}N_2O_8$	60,232	357.1809(1 0 0); 405.2013(28); 230.1385(23); 387.1923(18); 244.0955(12); 279.1703(10); 439.1565(8); 212.1297(7); 86.0971(7); 164.1068(7); 196.1348(6); 292.1175(6); 423.2108(6); 311.1724(4); 220.0978(4); 194.1176 (3); 127.0395(3); 136.0770 (2)
20	Fru-FL(I)	6.7	441.2224	441.2231	−1.66	$C_{21}H_{32}N_2O_8$	68,270	357.1813(1 0 0); 405.2022(43); 387.1933(27); 120.0814(27); 264.1245(25); 279.1717(15); 246.1129(10); 210.1119(10); 230.1184(8); 423.2119(8); 311.176(6); 198.0902(5); 369.1827(5); 291.1709(3); 86.0971(2)

(*continued on next page*)

Table 1 (*continued*)

ID	Compound Identity	RT	Exp. *m/z*	Calc. *m/z*	Error [ppm]	Mol. Formula	Intensity	Ion Fragments
21	Fru-FL(I)	4.7	441.2241	441.2231	2.14	$C_{21}H_{32}N_2O_8$	40,928	357.1799(1 0 0); 405.202(53); 264.1232(33); 120.0817(27); 387.1922(23); 279.1677(17); 246.1115(15); 230.1157(12); 311.1782(9); 423.2117(8); 210.1145(7); 369.1782(7); 291.1701(5); 198.0916(5); 86.098(4); 136.0762(3); 162.0936(3); 323.1751(3); 177.0578(3); 345.1789(2)
22	Glc-VY*	1.1	443.2021	443.2024	−0.66	$C_{20}H_{30}N_2O_9$	55,624	359.1601(1 0 0); 407.181(58); 389.1704(26); 216.1236(21); 280.1188(19); 281.1511(15); 136.075(11); 120.0819(11); 425.1889(10); 264.1229(8); 260.0907(8); 86.0968(6); 308.1144(6); 246.1138(5); 150.0909(5); 185.1669(5); 198.1142(5); 326.1211(4); 166.0874(4); 313.1521(4); 442.2366(4); 341.1482(3); 293.1507(2)
23	Fru-FE	1.1	457.1814	457.1817	0.66	$C_{20}H_{29}N_2O_{10}$	193,494	373.1397(1 0 0); 421.1615(50); 295.1275(23); 264.1211(21); 403.15(19); 120.0812(18); 439.1703(13); 246.1121(11); 226.0729(8); 274.0939(6); 198.0937(6); 148.0595(6); 228.1021(5); 310.1309(4); 355.1246(3); 327.1314(2); 307.1293(1)
24	Fru-MF	4.5	459.1797	459.1796	−0.22	$C_{20}H_{31}N_2O_8S$	74,878	375.1387(1 0 0); 423.1572(53); 248.0966(41); 292.1189(32); 405.1501(29); 212.0756(28); 104.0536(23); 244.0987(22); 297.1283(20); 230.0861(17); 441.17(14); 357.1358(12); 182.0629(11); 232.0975(10); 387.1351(7); 166.0851(7); 339.138(7); 274.1113(7); 307.1107(7); 129.1041(6); 200.0938(5); 367.1521(4); 327.1306(3); 258.0761(3); 309.1229(2)
25	Fru-VS	0.7	367.1709	367.1711	−0.69	$C_{14}H_{26}N_2O_9$	206,724	283.1299(1 0 0); 331.1506(33); 216.1248(32); 313.1405(19); 365.1058(11); 84.0821(10); 349.1589(10); 230.1381(9); 116.0706(9); 184.0605(9); 203.0541(8); 156.0738(6); 129.1023(6); 253.1293(6); 265.1202(6); 205.1199(4); 97.0293(4); 175.1123(4); 150.0941(3)
26	Fru-L(I)S or VT	0.7	381.1879	381.1868	3.03	$C_{15}H_{28}N_2O_9$	595,386	297.1458(1 0 0); 345.167(47); 216.1249(25); 327.1559(22); 230.1405(17); 363.1765(10); 219.1351(9); 212.1299(8); 86.0974(8); 150.0941(7); 136.0774(6); 198.0769(6); 231.1417(6); 309.1461(6); 279.1372(6); 258.1393(4); 120.0665(4); 232.0821 (3); 164.1092(3); 182.1179(3); 251.1064 (2)
27	Fru-V	0.7	280.1398	280.1391	2.70	$C_{11}H_{21}NO_7$	1,054,608	216.1245(1 0 0); 244.1185(60); 262.1296(46); 130.0872(28); 198.1133(21); 118.0875(18); 84.0823(12); 196.0976(10); 234.1343(10); 161.0694(9); 102.0922(9); 150.0925(8); 114.092(7); 154.0877(3); 110.0718(3); 180.1025(3); 156.1015(2); 226.107(2)
28	Fru-L(I)	0.7	294.1556	294.1547	3.11	$C_{12}H_{23}NO_7$	831,328	230.1398(1 0 0); 258.1349(55); 276.1445(38); 212.1288(21); 86.0977(18); 132.1027(13); 210.1135(12); 161.0683(11); 144.1031(11); 120.082(8); 97.0294(7); 248.1525(7); 220.084(4); 194.0473(2)
29	Fru-M	0.7	312.1114	312.1111	−0.96	$C_{11}H_{22}NO_7S$	138,344	276.0911(1 0 0); 230.0855(44); 84.0812(33); 248.0965(32); 133.0329(31); 88.04(25); 294.101(23); 228.0675(22); 104.0535(21); 150.058(18); 127.04(17); 118.0875(15); 212.0735(14); 258.0801(10); 220.0835(9); 97.0305(8); 200.0917(8); 143.0621(7); 161.0657(6); 111.0448(4); 192.0741(3); 266.1073(3); 181.0937(2); 162.0585(2)
30	Fru-F	1.0	328.1396	328.1391	2.39	$C_{15}H_{21}NO_7$	2,873,394	264.1243(1 0 0); 292.1191(88); 120.082(72); 310.1295(45); 132.0823(44); 244.0981(40); 166.0872(37); 246.1138(26); 178.0874(21); 161.0691(16); 127.0396(15); 143.0589(11); 198.0921(11); 97.0297(10); 228.1029(6); 282.1357(5); 112.0404(4); 204.1021(3); 232.0972(2); 274.108(2)
31	Fru-Y***	0.7	344.1345	344.1340	−1.58	$C_{15}H_{22}NO_8$	306,860	280.1187(1 0 0); 308.1133(75); 326.1232(62); 136.0759(27); 260.0924(20); 165.0566(17); 86.0971(15); 182.0821(13); 147.0775(13); 194.0822(13); 262.108(12); 130.0512(10); 234.1128(9); 97.0302(9); 107.0497(8); 248.0914(8); 217.0809(7); 298.131(6); 202.0757(5); 175.1174(5); 156.0672(4); 288.1098(4); 220.0968(3)
32	Fru-Y	0.8	344.1346	344.1340	−1.74	$C_{15}H_{22}NO_8$	727,500	280.1198(1 0 0); 308.1141(83); 326.1248(47); 165.0559(23); 136.0769(22); 260.0922(20); 148.0764(18); 262.1088(18); 86.0972(15); 194.0823(11); 182.0824(9); 107.0499(8); 123.0453(8); 97.0286(8); 244.1278(7); 214.0871(6); 298.1267(4); 234.1123(4); 202.0707(4); 224.0896(3)

Remaining structures have clear Amadori-specific fragmentation peaks, and the Heyns-specific peaks are less abundant or non-existent

* Heyns-specific peaks are more intensive than Amadori-specific peaks

** There are no either Amadori or Heyns-specific peaks

*** Splitting peak with different Amadori and Heyns-specific peaks than its counterpart (compound 32)

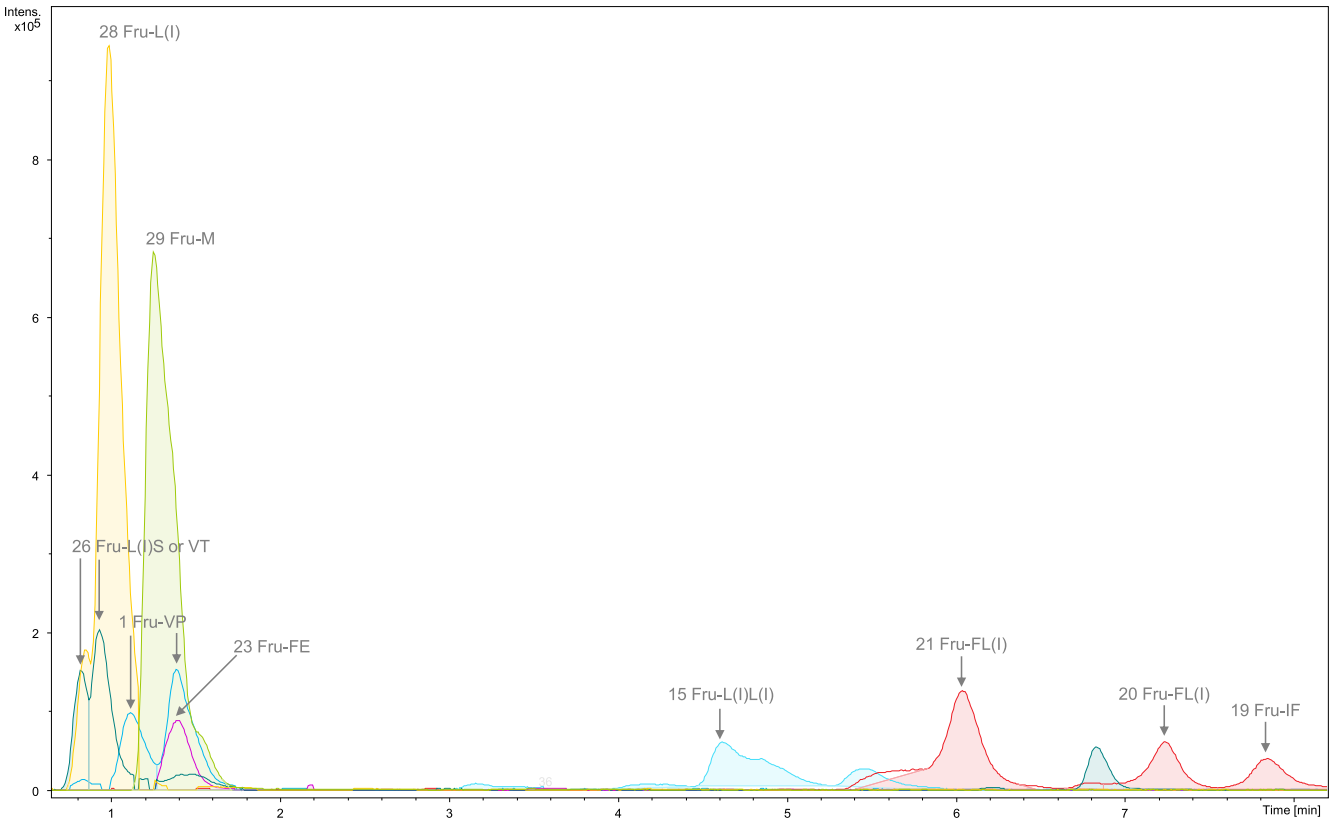

Fig. 2. Extracted ion chromatogram showing some of the identified Amadori compounds.

elucidation. Lastly, the bond between C_1 and C_2 carbon of the carbohydrate can break yielding the $[M-H+CH_2]^+$ ion (*m/z* 130), which confirms that the structure belongs to an amino acid and an aldohexose that underwent condensation and furtherly rearranged into the Amadori compound. Strangely enough, the spectrum contains a much smaller peak specific for Heyns compounds $[M+H\text{-}2H_2O\text{-}CH_3OH\text{-}CO]^+$ at *m/z* 156, which could be a result of the poor chromatographic resolution. The above-mentioned peaks derived from amino acid are mostly much less abundant than those resulting from the dehydration of the hexose. The fragmentation pattern matches a previously proposed fragmentation mechanism of N-glycosylated amino acids (Wang et al., 2008).

Additional amino acid causes the fragmentation pattern to be more complex. Still, the most abundant peaks for Fru-IT (Fig. 3b), *m/z* 395) are the ones originating from the dehydration of the hexose, but the ratio between individual peaks changes. Formation of the $[M+H\text{-}3H_2O\text{-}H_2CO]^+$ ion at *m/z* 311 is favored, and the decarboxylation does not occur for the $[M+H\text{-}H_2O]^+$ (*m/z* 377), $[M+H\text{-}2H_2O]^+$ (*m/z* 359), and $[M+H\text{-}3H_2O]^+$ (*m/z* 341) ions. Additionally, another dehydration can take place on the C-terminus of the peptide chain (*m/z* 323). On the other hand, Amadori-specific (*m/z* 245) and protonated peptide (*m/z* 233) peaks are not abundant, but other patterns arise as the fragmentation of both hexose and peptide components of the structure can break down at the same time. Most notably, a series of *a1* peptide fragments still attached to a hexose are present, alongside their sugar dehydration and decarboxylation products. Among them, the Sug-L(I)T *a1*-H_2O peak at *m/z* 230 was the most abundant (46% relative intensity). The specific *d* fragment ion at *m/z* 136 enabled us to confirm the presence of isoleucine moiety in the dipeptide. Besides other small peaks, three daughter ions contradicting our structure assignment were present (Fig. 3b), grayed out). Especially, the *m/z* 276 and 198 peaks containing *y1* peptide fragments attached to hexoses, which could not be formed without some unlikely rearrangement.

Unsurprisingly, the N-glycosylated tripeptide Glc-TVW (Fig. 3c), *m/z* 567), exhibit the most complex fragmentation pattern. The sugar component degradation behavior is similar to the one displayed by the previous dipeptide, but the relative intensity of the peaks decreased with respect to the rest of the spectra. The $[M+H\text{-}3H_2O\text{-}H_2CO]^+$ ion at *m/z* 483 is not the most abundant fragment. Heyns-specific peak, as well as the protonated peptide, is smaller, but present (*m/z* 471 and 405 respectively). The most abundant peak in the spectra is a *y2* peptide fragment of either TVW or TWV at *m/z* 304, followed by the Sug-**W *b2*-$2H_2O$-CO at *m/z* 299. Most of the remaining daughter ions originate from the *b2* fragment ion and fragmentation of the protonated peptide. Additionally, there are also three peaks not conforming to our expectations, similarly to the previously described dipeptide.

The collision energy depended on the mass of individual parent ion, but still, all the compounds in this study were fragmented in similar conditions (energy between 26 and 34 eV). Although only the twenty-three-dipeptide group is large enough to derive some general pattern of behavior. Still, we have identified six N-glycosylated amino acids known in cocoa, twenty-three N-glycosylated dipeptides, and three N-glycosylated tripeptides that were previously unreported. Twenty-three of them are undoubtedly Amadori compounds (**1–3**, **5**, **7–9**, **14–17**, **20**, **21**, **23–32**), four Heyns compounds (**4**, **11**, **13**, **22**), and five lack distinguishing fragments but were assigned as Amadori compounds (**6**, **10**, **12**, **18**, **19**). Recent literature does not indicate that the analytical standards of Amadori compounds can fragment producing Heyns-specific peaks. In total, nineteen were ambiguously assigned because of unclear peptide sequence or lack of Amadori- or Heyns-specific peaks (**see** Table 1).

Each type of N-glycosylated species in this study is clearly distinguishable from each other (see Fig. 3 and Supplementary Information). The single amino acids containing compounds have the simplest fragmentation spectra among all and exhibit a particular pattern of the hexose-specific dehydration and decarboxylation. In most of them (the only exception is Fru-M, **29**), the most abundant peak is the $[M+H\text{-}2H_2O\text{-}CO]^+$ ion. The amino acid part-specific peaks are not abundant

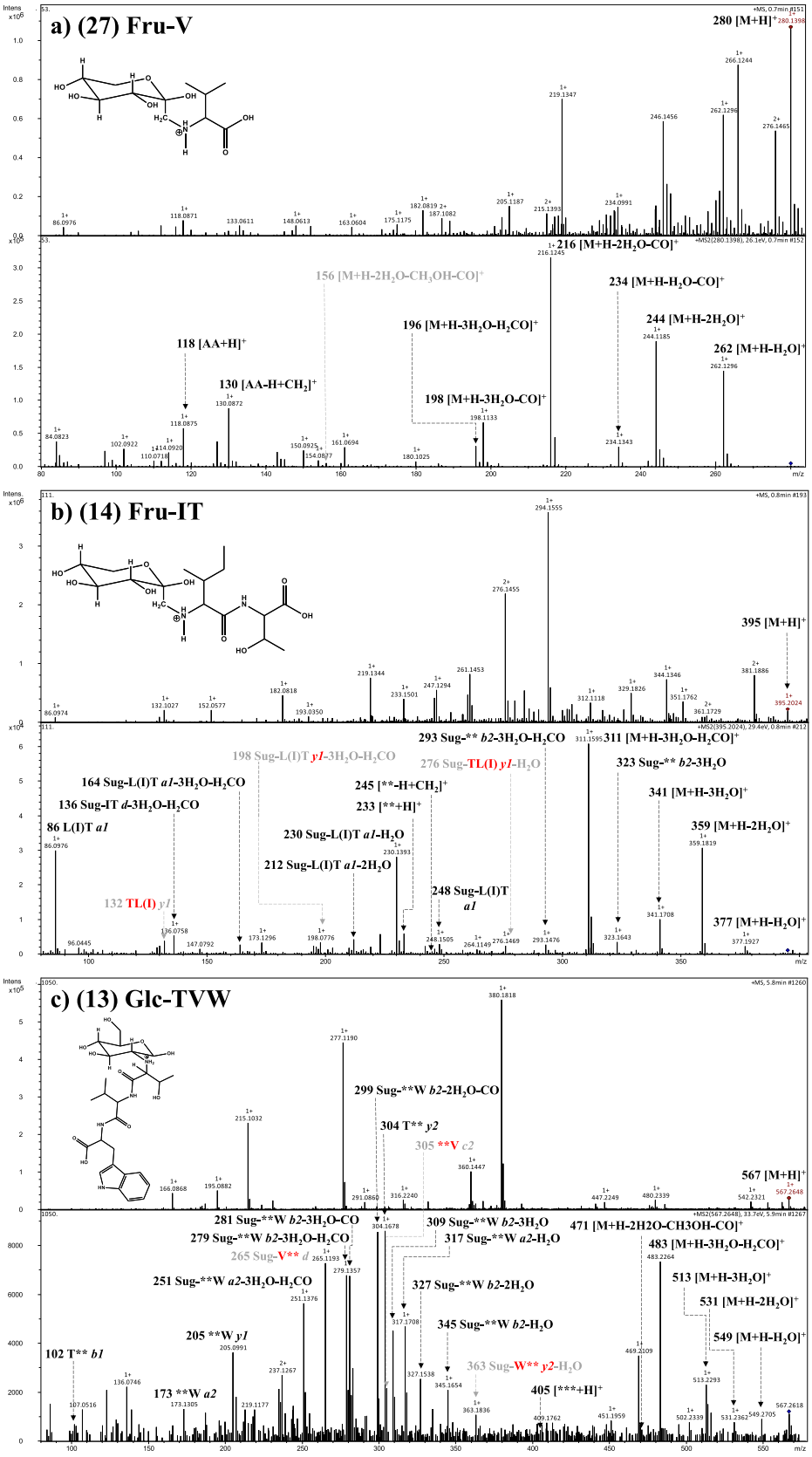

Fig. 3. An example of HPLC-ESI-MS-MS fragmentation spectra of N-glycosylated peptides for a) (27) Fru-V, b) (14) Fru-IT, and c) (13) Glc-TVW, Fru- being fructosyl (Amadori compound), and Glc- glycosyl- (Heyns compound) species respectively. All important ion fragments (> 1% relative intensity) are annotated. "AA" and "*" indicate any single amino acids that are part of the individual structures. Letters and numbers in italics (e.g., *a1*) are the notations based on the standard peptide fragmentation nomenclature. Grayed-out text indicates fragments specific to other isomers of the elucidated structure, while the red highlights point out how those peaks contradict our assignment. L(I) annotation implies that the fragment is the same for both leucine and isoleucine.

and are limited only to the protonated amino acid peak $[AA + H]^+$. In the case of dipeptide Amadori and Heyns compound, the spectra change slightly. Still, the peptide degradation occurs in a smaller degree, and the main peaks produced belong to the hexose degradation. However, the ratio between the hexose peaks changes, with the most abundant one being the $[M + H\text{-}3H_2O\text{-}H_2CO]^+$ for most cases, except the proline-containing compounds. Fru-VP (**1**) and Fru-L(I)P (**8**) display the Sug-VP *a1*-H_2O and the $[M + H\text{-}3H_2O\text{-}CO]^+$ as the most abundant

peaks, respectively. As the length of the amino acid chain increase by one, the variety of the peptide-specific fragments increases. This is true for the tripeptides, as well. In their case, the hexose degradation pattern is very similar, but the most abundant peaks are the ones that combine both hexose and peptide fragmentations. The complexity of spectra dramatically increases.

Additionally, we have identified some irregularities in the behavior of most of the presented compounds during HPLC-ESI-MS-MS fragmentation. First of all, the differentiation between Amadori and Heyns compounds was ambiguous in some cases. Only nineteen from thirty-two compounds had obvious fragments of either Amadori or Heyns compounds. Surprisingly, seven had both of them (**2**, **4**, **21**, **25**, **27**, **30**, **31**), and six none of them (**6**, **10**, **12**, **15**, **18**, **19**). This behavior is not clear, and literature does not indicate that it occurs for MS-MS fragmentation of analytical standards. Secondly, most di- and tripeptide-containing structures produced fragments that would indicate a different sequence of amino acids in the peptide chain that suggested by other daughter ions (e.g., Fig. 3b), *m/z* 132). However, those peaks appear infrequently; therefore, they did not affect our assignment. Their appearance in the spectra would have to be associated with either poor chromatographic resolution of different isomers, or an unlikely rearrangement. Finally, in some cases of di- and tripeptide-containing structures, an ion comprised of *y* peptide fragment and hexose fragment is produced (e.g., Fig. 3b), *m/z* 276, and 198). This is highly unexpected, as the formation of *y* ions would mean that the peptide part of the compound broke off the hexose part. There is no clear explanation for this behavior.

3.2. Discriminant analysis of different cocoa samples based on Amadori compound content

Employing both reported previously and newly identified Amadori and Heyns compounds, discriminant analysis was performed, which successfully distinguished the samples based on their geographical origin (see PCA in Fig. 4). At first, all the chemical species were included, however, using only the top 14 most important features (ranked by InfoGain method of Orange software) improved the separation. The principal component analysis distinguishes African countries very well, even among themselves. The Brazilian sample stood out as well, most likely because of bad weather conditions during the year of the harvest. The rest of the samples separate as well, yet it is difficult to speculate why without including more samples from each of the regions. Most notably, the separation based on origins is doubtlessly affected by a variety of the cocoa hybrid as well as post-harvest practices (such as drying and fermentation), and those should be taken into account in further studies.

Fig. 5 shows bar charts of chosen Amadori compounds and their putative peptide precursors for some of the samples presented in the study. There seems to be a slight connection between the Amadori compound content and their corresponding peptides; however, this result furtherly enforces the earlier point, that the important factors shaping the Amadori content profile of cocoa are the hybrid type and the fermentation and drying. Unfortunately, our data lack this basic information for most of the samples. Nevertheless, there are significant differences in Amadori and Heyns compounds content between the presented samples. Additionally, considering the well-known fundamental involvement of these compounds in aroma and color formation in heated foods. novel compounds described herein should be considered as important markers of cocoa quality and origin. However, direct links between aroma quality and presented compounds have yet to be established.

4. Conclusions

In our study, we have identified thirty-two N-glycosylated short-peptides (Amadori and Heyns compounds), of which twenty-six are novel to cocoa. We have demonstrated their general ESI-MS-MS fragmentation patterns, which agree with previous findings in the literature. Additionally, we have described some unusual daughter ions that occur in many of the presented compounds, which should be confirmed by experiments on authentic analytical standards. Our data shows that there is more variety in Amadori compounds in cocoa (and in food) than it was reported so far. We believe that further studies on these compounds can shed some light on chemical transformations occurring during cocoa processing. Moreover, we have relatively quantified all presented species in thirteen samples of cocoa originating from different countries. The principal component analysis has shown that these samples have different Amadori compound profiles, and it is possible to distinguish them on this basis alone, which suggests they could be an important quality marker. Nevertheless, further research is necessary as it could be a result of different fermentation and drying practices as well as a variety of cocoa. Still, we believe this research

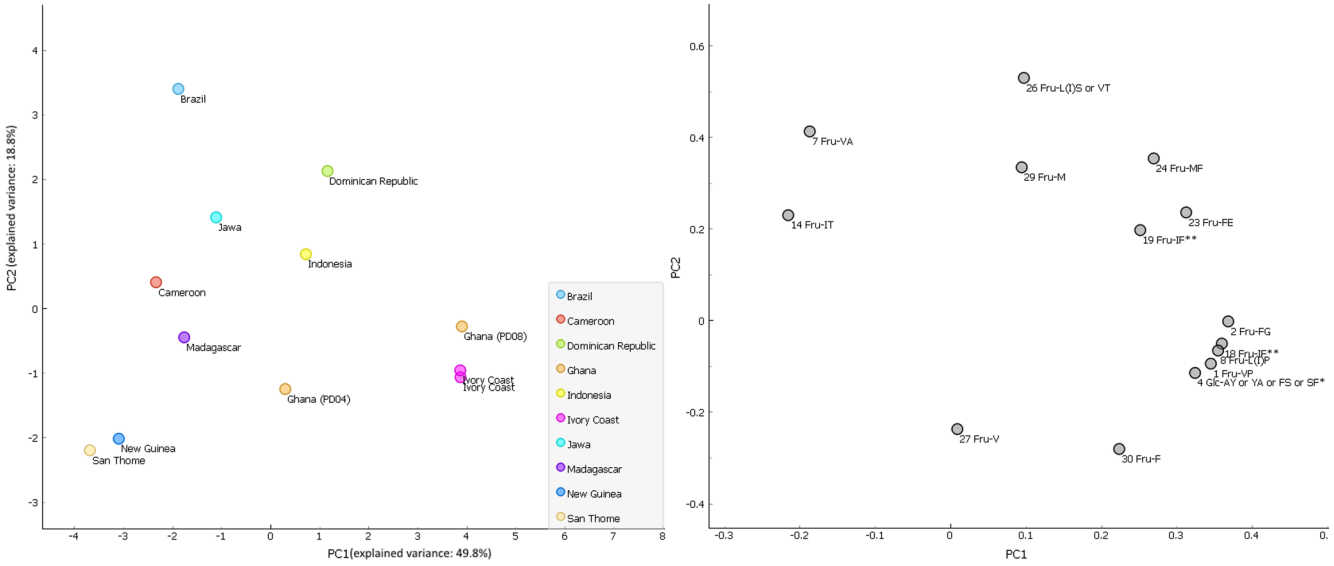

Fig. 4. Principal component analysis of dry cocoa beans from different origins based on their Amadori and Heyns compounds content (explained variance: PC1 49.8%; PC2 18.8%).

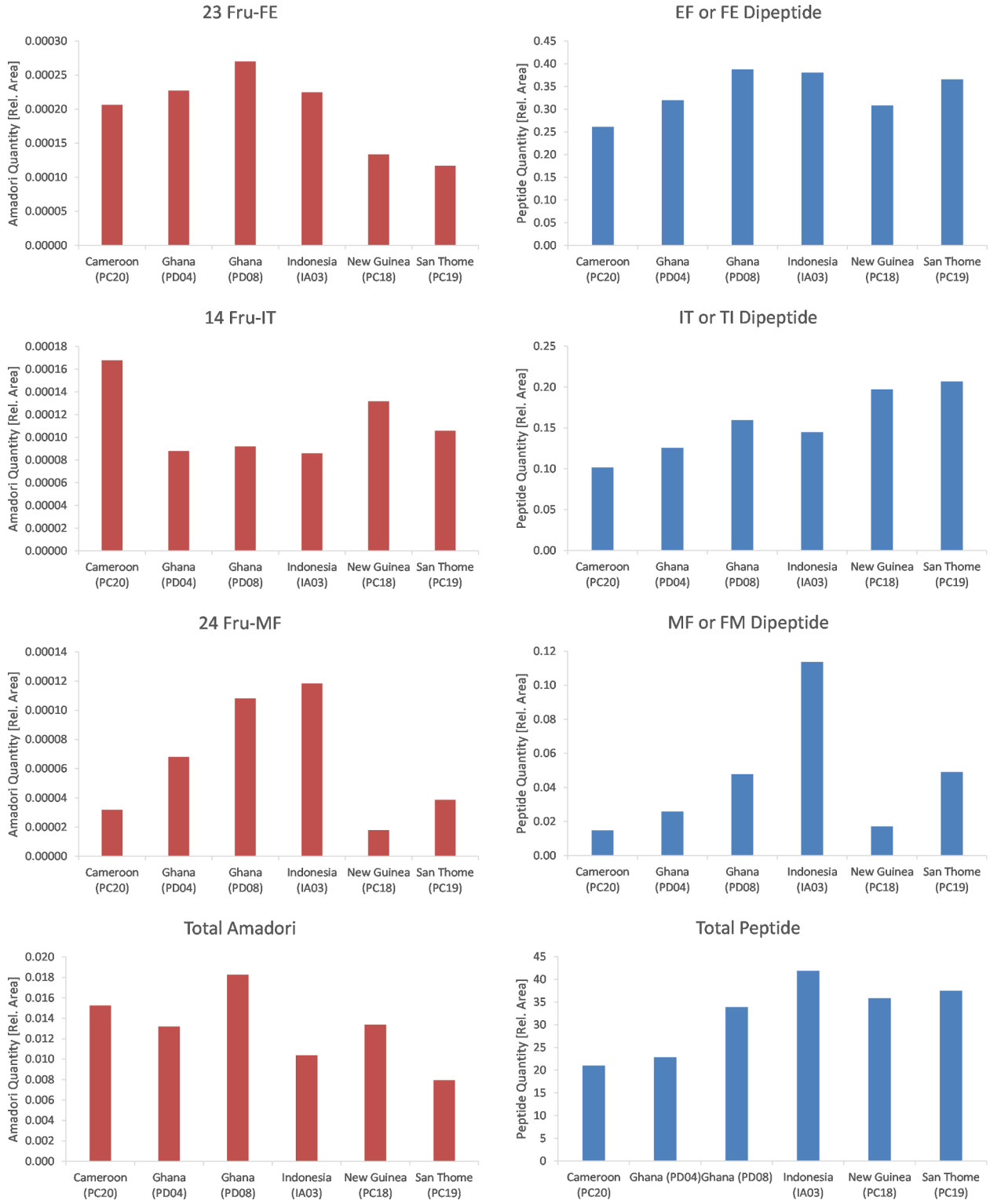

Fig. 5. Relative quantities of some of the Amadori compounds (left) and their putative peptide precursors (right) for chosen countries of origin.

provides groundwork for the identification of further Amadori and Heyns compounds, as well as linking them to the quality and origin of different cocoa beans.

Acknowledgments

We thank Britta Behrends for technical support in HPLC-MS measurements.

Funding

This work was conducted in the framework of the COMETA Project, which is financially supported by Barry Callebaut AG.

Conflict of interest statement

The authors of this research paper receive research funding from

Barry Callebaut. The terms of this arrangement have been reviewed and approved by the Jacobs University Bremen in accordance with its policy on objectivity in research.

Appendix A. Supplementary data

Supplementary data to this article can be found online at https://doi.org/10.1016/j.foodres.2020.109164.

References

Ames, J. M. (1990). Control of the Maillard reaction in food systems. *Trends in Food Science & Technology, 1*, 150–154. https://doi.org/10.1016/0924-2244(90)90113-D.

Ames, J. M. (1998). Applications of the Maillard reaction in the food industry. *Food Chemistry, 62*(4), 431–439. https://doi.org/10.1016/S0308-8146(98)00078-8.

Beckett, S. T. (Ed.). (2009). *Industrial chocolate manufacture and use*(4. ed). Oxford: Wiley-Blackwell.

Camu, N., De Winter, T., Addo, S. K., Takrama, J. S., Bernaert, H., & De Vuyst, L. (2008). Fermentation of cocoa beans: Influence of microbial activities and polyphenol concentrations on the flavour of chocolate. *Journal of the Science of Food and Agriculture, 88*(13), 2288–2297. https://doi.org/10.1002/jsfa.3349.

Coursey, J. S., Schwab, D. J., Tsai, J. J., & Dragoset, R. A. (2015). Atomic weights and isotopic compositions (version 4.1). Retrieved August 22, 2018, from NIST website: http://physics.nist.gov/Comp.

Davidek, T., Clety, N., Aubin, S., & Blank, I. (2002). Degradation of the Amadori Compound N-(1-Deoxy-d-fructos-1-yl)glycine in Aqueous Model Systems. *Journal of Agricultural and Food Chemistry, 50*(19), 5472–5479. https://doi.org/10.1021/jf025561j.

Davidek, T., Kraehenbuehl, K., Devaud, S., Robert, F., & Blank, I. (2005). Analysis of Amadori Compounds by High-Performance Cation Exchange Chromatography Coupled to Tandem Mass Spectrometry. *Analytical Chemistry, 77*(1), 140–147. https://doi.org/10.1021/ac048925a.

Demsar, J., Curk, T., Erjavec, A., Gorup, C., Hocevar, T., Milutinovic, M., ... Zupan, B. (2013). Orange: Data Mining Toolbox in Python. *Journal of Machine Learning Research, 14*, 5.

D'Souza, R. N., Grimbs, A., Grimbs, S., Behrends, B., Corno, M., Ullrich, M. S., & Kuhnert, N. (2018). Degradation of cocoa proteins into oligopeptides during spontaneous fermentation of cocoa beans. *Food Research International, 109*, 506–516. https://doi.org/10.1016/j.foodres.2018.04.068.

Eichner, K., Reutter, M., & Wittmann, R. (1993). Detection of Amadori Compounds in Heated Foods. In T. H. Parliment, M. J. Morello, & R. J. McGorrin (Eds.), Thermally Generated Flavors (Vol. 543, pp. 42–54). Doi: 10.1021/bk-1994-0543.ch005.

Hau, J., Devaud, S., & Blank, I. (2004). Detection of Amadori compounds by capillary electrophoresis coupled to tandem mass spectrometry. *Electrophoresis, 25*(13), 2077–2083. https://doi.org/10.1002/elps.200405958.

Hofmann, T., & Schieberle, P. (2000). Formation of Aroma-Active Strecker-Aldehydes by a Direct Oxidative Degradation of Amadori Compounds. *Journal of Agricultural and Food Chemistry, 48*(9), 4301–4305. https://doi.org/10.1021/jf000076e.

Horvat, Š., & Jakas, A. (2004). Peptide and amino acid glycation: New insights into the Maillard reaction. *Journal of Peptide Science, 10*(3), 119–137. https://doi.org/10.1002/psc.519.

Jeri?, I., Versluis, C., Horvat, ?tefica, & Heck, A. J. R. (2002). Tracing glycoprotein structures: electrospray ionization tandem mass spectrometric analysis of sugar-peptide adducts. Journal of Mass Spectrometry, 37(8), 803–811. Doi: 10.1002/jms.337.

Lagunes Gálvez, S., Loiseau, G., Paredes, J. L., Barel, M., & Guiraud, J.-P. (2007). Study on the microflora and biochemistry of cocoa fermentation in the Dominican Republic. *International Journal of Food Microbiology, 114*(1), 124–130. https://doi.org/10.1016/j.ijfoodmicro.2006.10.041.

Megías-Pérez, R., Grimbs, S., D'Souza, R. N., Bernaert, H., & Kuhnert, N. (2018). Profiling, quantification and classification of cocoa beans based on chemometric analysis of carbohydrates using hydrophilic interaction liquid chromatography coupled to mass spectrometry. *Food Chemistry, 258*, 284–294. https://doi.org/10.1016/j.foodchem.2018.03.026.

Meitinger, M., Hartmann, S., & Schieberle, P. (2014). Development of Stable Isotope Dilution Assays for the Quantitation of Amadori Compounds in Foods. *Journal of Agricultural and Food Chemistry, 62*(22), 5020–5027. https://doi.org/10.1021/jf501464g.

Mennella, C., Visciano, M., Napolitano, A., Castillo, M. D. D., & Fogliano, V. (2006). Glycation of lysine-containing dipeptides. *Journal of Peptide Science, 12*(4), 291–296. https://doi.org/10.1002/psc.722.

Rodriguez-Campos, J., Escalona-Buendía, H. B., Contreras-Ramos, S. M., Orozco-Avila, I., Jaramillo-Flores, E., & Lugo-Cervantes, E. (2012). Effect of fermentation time and drying temperature on volatile compounds in cocoa. *Food Chemistry, 132*(1), 277–288. https://doi.org/10.1016/j.foodchem.2011.10.078.

Ruan, D., Wang, H., & Cheng, F. (2018). The Maillard Reaction in Food Chemistry: Current Technology and Applications. Retrieved from https://www.springer.com/gp/book/9783030047764.

Singh, R., Barden, A., Mori, T., & Beilin, L. (2001). Advanced glycation end-products: A review. *Diabetologia, 44*(2), 129–146. https://doi.org/10.1007/s001250051591.

Wang, J., Lu, Y.-M., Liu, B.-Z., & He, H.-Y. (2008). Electrospray positive ionization tandem mass spectrometry of Amadori compounds. *Journal of Mass Spectrometry, 43*(2), 262–264. https://doi.org/10.1002/jms.1290.

Yaylayan, V. A. (2003). Recent Advances in the Chemistry of Strecker Degradation and Amadori Rearrangement: Implications to Aroma and Color Formation. *Food Science and Technology Research, 9*(1), 1–6. https://doi.org/10.3136/fstr.9.1.

Yuan, H., Sun, L., Chen, M., ... Wang, J. (2016). The Comparison of the Contents of Sugar, Amadori, and Heyns Compounds in Fresh and Black Garlic: Comparison of compounds in black garlic.... *Journal of Food Science, 81*(7), C1662–C1668. https://doi.org/10.1111/1750-3841.13365.

Yuan, H., Sun, L., Chen, M., & Wang, J. (2017). The Simultaneous Analysis of Amadori and Heyns Compounds in Dried Fruits by High Performance Liquid Chromatography Tandem Mass Spectrometry. *Food Analytical Methods, 10*(4), 1097–1105. https://doi.org/10.1007/s12161-016-0669-1.

Zou, T., Liu, J., Song, H., & Liu, Y. (2018). Discovery of Amadori-Type Conjugates in a Peptide Maillard Reaction and Their Corresponding Influence on the Formation of Pyrazines. *Journal of Food Science, 83*(6), 1588–1595. https://doi.org/10.1111/1750-3841.14156.